Fırat Üniversitesi Müh. Bil. Dergisi
37(1), 341-350, 2025

Araştırma Makalesi
https://doi.org/10.35234/fumbd.1557122

Deep Analysis of Patella caerulea Calcined Shells for Microwave Applications

Erkan UĞURLU[1], Muharrem KARAASLAN[2], Fatih Özkan ALKURT[2*], Kerim Emre ÖKSÜZ[3], Önder DUYSAK[4]

[1]Faculty of Science and Letters, Chemistry Department, Çukurova University, Adana, Türkiye
[2]Electrical and Electronics Eng. Iskenderun Technical University, Iskenderun, Hatay, Türkiye
[3]Sivas Cumhuriyet University, Department of Metallurgical and Materials Engineering, Sivas, Türkiye
[5]Faculty of Marine Science and Technology, Iskenderun Technical University, Iskenderun, Hatay, Türkiye
[1]erkn.ugurlu@yahoo.com, [2]muharrem.karaaslan@iste.edu.tr, [*3]fozkan.alkurt@iste.edu.tr,
[4]emre.oksuz@cumhuriyet.edu.tr, [5]onder.duysak@iste.edu.tr

(Geliş/Received: 27/09/2024; Kabul/Accepted: 12/03/2025)

Abstract: This study investigates the potential application of Patella caerulea shells collected from the Iskenderun Bay as biomaterial in microwave radomes and examines the dielectric properties of shells calcined at 600-1200 °C. At the central frequency of 10 GHz, the real permittivity values for P600, P800, P1000 and P1200 are 3.2, 2.3, 2.4 and 2.5, respectively. The corresponding imaginary parts at 10 GHz are 0.82, 0.44, 0.52 and 0.56, reflecting temperature-dependent variations. The loss factor of shells, particularly at 2.5 GHz, indicates their potential for low-loss applications in communication, such as microwave laminate and radome applications. Moreover, these materials have been integrated to a traditional patch antenna to show feasibility in a microwave system as a substrate layer. At temperatures exceeding 800 °C, slight increase in the CaO peaks was observed in X-ray diffraction spectrum. The thermal gravimetric analysis and differential thermal analysis of shell powder reveal weight loss occurring in two distinct stages and minor endothermic peaks at 125°C and 275°C. The study highlights that microwave antenna radome materials are promising due to their high impedance matching and low-loss properties. This research contributes to the exploration of marine-sourced materials for economic and ecological benefits in the field of microwave technology.

Key words: Dielectric, Marine materials, Characterization, Microwave, Limpets.

Patella caerulea Kalsine Kabuklarının Mikrodalga Uygulamaları İçin Derinlemesine Analizi

Öz: Bu çalışma, İskenderun Körfezi'nden toplanan Patella Caerulea kabuklarının mikrodalga radomelarında biyomalzeme olarak potansiyel uygulamasını araştırmakta ve 600-1200 °C'de kalsine edilmiş kabukların dielektrik özelliklerini incelemektedir. 10 GHz'lik merkezi frekansta, P600, P800, P1000 ve P1200 için reel dielektrik geçirgenlik değerleri sırasıyla 3,2, 2,3, 2,4 ve 2,5'tir. 10 GHz'de karşılık gelen sanal değerleri, sıcaklığa bağlı değişimleri yansıtan 0,82, 0,44, 0,52 ve 0,56'dır. Kabukların, özellikle 2,5 GHz'deki kayıp faktörü, mikrodalga laminat ve radome uygulamaları gibi iletişimde düşük kayıplı uygulamalar için potansiyellerini göstermektedir. Ayrıca, bu malzemeler bir mikrodalga sistemde alt tabaka olarak uygulanabilirliğini göstermek için geleneksel bir yama antene entegre edilmiştir. Bununla birlikte, 800 °C'yi aşan sıcaklıklarda X-ışını kırınım spektrumunda CaO tepelerinde hafif bir artış gözlemlenmiştir. Kabuk tozunun termal gravimetrik analizi ve diferansiyel termal analizi, iki ayrı aşamada oluşan ağırlık kaybını ve 125 °C ve 275 °C'de küçük endotermik tepeleri ortaya koymaktadır. Çalışma, mikrodalga anten radom malzemelerinin yüksek empedans uyumu ve düşük kayıp özellikleri nedeniyle umut verici olduğunu vurgulamaktadır. Bu araştırma, mikrodalga teknolojisi alanında ekonomik ve ekolojik faydalar için deniz kaynaklı malzemelerin keşfine katkıda bulunmaktadır.

Anahtar kelimeler: Dielektrik, deniz malzemeleri, karakterizasyon, mikrodalga, deniz salyangozları.

1. Introduction

Limpets of the genus Patella are gastropods that graze in rocky areas in the middle and upper-lower coastal regions of the Atlantic and Mediterranean coasts in temperate regions [1]. It has an important role in the ecological and biological control of algae, that is the species distributed in coastal areas [2,3]. They are known as keystone species in the mid-littoral point of the coastal regions and are rarely consumed by humans and used as fish food [4]. Limpets are species that increase or decrease the amount of macroalgae species and the availability of other marine organisms. It also has an important position as the species that forms and regulates the ecological balance of tidal communities [2,5,6]. In the Mediterranean region, the Patella genus has four different species. These are

* Sorumlu yazar: fozkan.alkurt@iste.edu.tr. Yazarların ORCID Numarası: [1]0000-0001-8940-8421, [2]0000-0003-0923-1959, [2]0000-0002-9940-0658, [3]0000-0001-7424-5930, [4]0000-0002-7484-3102

P. caerulea, *P. ulyssiponensis, P. rustica* and *P. ferruginea*. *P. caerulea* which is known as a native Mediterranean limpet (Linnaeus, 1758) is found on cliffs or between rocky areas in the infralittoral and midlittoral regions of the Mediterranean coast [7]. It is considered as an endemic (native) species in the Mediterranean region [8–10].

There are many studies on the biology, distribution, ecology, population characteristics, chitin and chitosan production and availability of Patella species in the Eastern Mediterranean coast [11–18]. In the literature, a study was found in which the shells of invasive sea urchin were investigated using radome technology [19]. Radome technology studies need to be focused on marine-based animals, and these materials which are currently found in nature as waste, and especially those that do not have economic importance, need to be brought into the economy. In this way, both ecological and economic benefits will be provided. Especially in recent years, studies have been carried out on the integration of marine origin materials into different multidisciplinary fields. The most important features of marine-sourced materials are that they are non-toxic, biodegradable and compatible [20].

Furthermore, a "radome" is a structure that protects a radar system or other sensitive electronic equipment from the environment while allowing the electromagnetic signals to pass through with low reduction and scattering [21]. The term "radome" is the combination of the term "radar" and "dome" that is aimed to be transparent to the frequencies used by the radar system. There are many aspects of the radome theory. For example, it protects radar antennas and other sensitive equipment from environmental factors such as rain, wind, snow, and temperature extremes. They also shield against physical damage and corrosive elements, helping to extend the lifespan of the radar system. Moreover, they are designed to be transparent to the radio frequency signals used by radar systems. This allows the radar beams to pass through the radome without significant distortion, ensuring that the performance of the radar system is not compromised. Radome structures can be used in many applications such as military radars [22], weather radar [23], air traffic control radar [24] and satellite communications [25]. Finally, radomes are essential for upholding the effectiveness and dependability of radar systems, serving as safeguarding and transparent enclosures for sensitive electronic components.

This study is the first to explore the potential of Mediterranean limpet *Patella caerulea* shells, abundantly found along the Turkish coasts, as a biomaterial for microwave applications, particularly in radome structures. Unlike previous research, which has not investigated the applicability of *P. caerulea* seashells in microwave systems, this study provides a comprehensive analysis of their dielectric properties after calcination at different temperatures. The constitutive parameters of the calcined shells were extracted through microwave measurements, offering valuable insights into their feasibility for electromagnetic applications. To further demonstrate their practical implementation, a traditional patch antenna was designed and numerically analyzed with the proposed biomaterial integration. Additionally, an extensive characterization process was conducted, including morphological analysis via Scanning Electron Microscopy (SEM), crystallographic investigation using X-ray diffraction (XRD), and thermal stability assessment through Thermogravimetric Analysis (TGA) and Derivative Thermogravimetry (DTG). This multidisciplinary approach underscores the innovative use of *P. caerulea* shells as a sustainable and effective material in microwave engineering, filling a significant gap in the literature.

2. Preparation of Samples

Patella caerulea used in the invention of biomaterials has been collected from the Iskenderun Bay. All soft tissues were removed. Then, the shell thoroughly washed with tap water and then with bidistilled water and dried in an oven at 50 °C for 24 h (Fig. 1). The dried biomaterials were ground and sieved with the help of a grinder (Fig. 2).

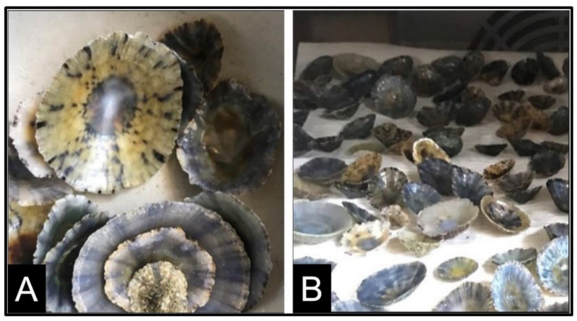

Figure 1. *P. caerulea* shells: A) washed distilled water and B) dried in oven.

A method by Park et al. [26] was modified to calcine dried shell powders at four different temperatures (600, 800, 1000 and 1200 °C) in a 1200 °C muffle furnace (Protherm-Furnaces) for 1 hour, with a heating rate of 5 °C/min. The calcined materials were left to dry in the desiccator. Immediately afterwards, the shell powder biomaterial was labeled as P600, P800, P1000 and P1200. It was kept in closed falcon tubes to be used in experiments to measure electromagnetic properties in microwave analysis. After these processes, microwave analysis has been started.

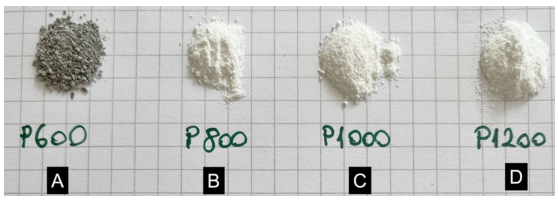

Figure 2. Images of calcined *P. caerulea* powder shells at different temperatures: A) 600 °C, B) 800 °C, C) 1000 °C and D) 1200 °C.

3. Sample Characterization

X-ray diffraction (XRD) analysis was performed to determine the mineral composition of the calcined *P. caerulea* shells. XRD analysis was carried out using an X-ray diffractometer [Malvern Panalytical EMPYREAN 3rd Generation Analytical (UK)] equipped with Ni-filtered Cu-Kα radiation operating at 40 kV and 30 mA. The data were collected over a 2θ range from 5° to 90°, with intervals of 0.02° and a counting time of 1 second per step. The measurements were conducted at the Central Laboratory of Iskenderun Technical University. The surface morphology and microstructures of the calcined shell powder samples were examined using Scanning Electron Microscopy (SEM, JEOL JSM-6380LA) operating at 10 kV. Prior to imaging, the samples were coated with a gold-palladium (Au-Pd) alloy using the POLARON SC7620 sputter coater to enhance their conductivity and improve image quality. Thermogravimetric analysis (TGA) and derivative thermogravimetry (DTG) are crucial for assessing the thermal properties, stability, and composition of shell samples. These analyses enable researchers and industry professionals to make informed decisions about material thermal properties and thermal performance. To examine the thermal and degradation profiles of the collected and prepared shell samples, TGA/DTG was conducted using a DTG 60 series TG/DTA thermal analyzer (Shimadzu, Japan). The samples were scanned at a rate of 10 °C per minute in an air atmosphere, covering a temperature range from 50 °C to 1000 °C. Measurements were taken in triplicate using a sample mass of 4 mg [27].

4. Microwave Analysis

Microwave laboratory analysis was conducted on meticulously prepared shell powder samples, wherein the complex permittivity parameters for each sample were determined by utilizing a dielectric probe kit and an Agilent PNLA Vector Network Analyzer (VNA), as illustrated in Fig. 3A by using open ended coaxial prob method. The investigation into the potential microwave applications of these samples spanned a broadband frequency range from 1 GHz to 20 GHz and all measurements have been carried out in room temperature. Despite the availability of various techniques for determining the relative permittivity, the open-ended coaxial probe method was specifically chosen due to the powdered form of the samples. The complex dielectric parameter of a material is expressed in terms of the relative permittivity in Eq. (1) [28];

$$\varepsilon = \frac{P}{\varepsilon_0 E} + 1 \tag{1}$$

where P is the polarization with respect to the electrical field strength and E of an external electric field. The relative complex dielectric constant of the sample was calculated according to Eq. (2) [29];

$$\varepsilon = \varepsilon' - j\varepsilon'' \tag{2}$$

The loss tangent is determined according to Eq. (3) [29];

$$\tan\delta = \frac{\varepsilon''}{\varepsilon'} \quad (3)$$

Prior to conducting measurements, a calibration procedure was meticulously executed to mitigate losses, minimize noise, and alleviate potential interferences arising from laboratory conditions. The measurement frequency range was strategically set between 1 GHz and 20 GHz, encompassing the maximum dielectric parameter band of the utilized Vector Network Analyzer (VNA). The dielectric probe kit is conducted to a three-fold calibration process. Initially, the probe kit was tested under an open-ended line, measuring air at room temperature (Fig. 3B). Subsequently, a shorting block was affixed to the end of the probe line, inducing a short circuit effect on the primary microwave line (Fig. 3C). Finally, the probe line was connected to a clean water tube under room temperature conditions, serving as a reference sample for calibration (Fig. 3D). Notably, the dielectric characteristics of water and air, being well-established, facilitated the use of measured values from these samples to verify the calibration accuracy.

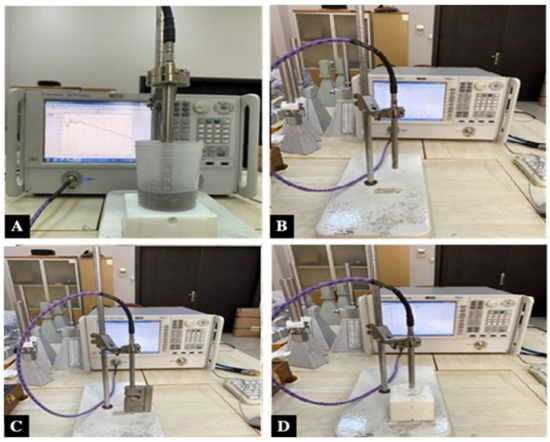

Figure 3. (A) Complex dielectric parameter measurement setup for 1 GHz-20 GHz band, (B) Calibration with respect to air, (C) known load and (D) pure water.

5. Scanning Electron Microscopy (SEM) Analysis

Shell samples of *P. caerulea* were collected from rocks along the shores of the İskenderun Bay. These samples were subsequently cleaned, ground, and calcined at temperatures ranging from 600°C to 1200°C. Scanning Electron Microscopy (SEM) analysis was conducted on the calcined shell powders, as shown in Fig. 4. Morphological changes in the *P. caerulea* shell powder were observed at four different calcination temperatures using SEM. To provide a more comprehensive understanding of the morphological structures, SEM photos were captured at various magnifications.

The SEM photo of the sample obtained from *P. caerulea* shell powders calcined at 600°C reveals a broader view of the shell's surface, displaying a rough and porous texture indicative of insufficient thermal decomposition and phase changes due to the low calcination temperature (Figs. 4A and 5B). The image taken at higher magnification shows more distinct grain boundaries in the microstructure. The photograph taken at the lowest temperature shows a highly irregular spherical/layered porous surface. However, it should be noted that the calcination temperature of 600°C is insufficient to achieve complete thermal decomposition of the *P. caerulea* shells material. Higher temperatures are required to fully transform the material and achieve more uniform microstructural changes. The microstructure of the powders showed larger particles of irregular shape and non-uniform size distribution, which could be related to the unreacted $CaCO_3$. The microstructures of powders calcined at 800°C show irregularly shaped, clustered structures like those at 600°C, but with a higher degree of thermal decomposition compared to 600°C (Figs. 4C-D). The rough and porous texture is observed at all calcination temperatures, as identified from the SEM images. It was also observed that laminated CaO crystals formed within the structure as the calcination temperature increased.

In contrast, the surfaces of the calcined *P. caerulea* shells, as observed in Figs. 4E-6F, exhibited a fluffy-like structure. It was noted that at temperatures above 600°C, all traces of organic macromolecules such as proteins and polysaccharides in the shell powder disappeared completely, leaving the structure devoid of these components. As the calcination temperature increased, the release of CO_2 gas during the conversion from calcium carbonate to CaO led to significant pore formation within the structure. SEM photographs at temperatures of 1000°C and above indicated the absence of the $CaCO_3$ phase in the crystal structure post-calcination (Figs. 4E and F), confirming its complete transformation into a single phase (CaO), which was further corroborated by XRD analyses. Significant differences between CaO powders and $CaCO_3$ powders were observed. Specifically, in *P. caerulea* shell powders subjected to calcination at 1000 and 1200 °C, the structure underwent a complete transformation into crystalline CaO, distinguishing it from samples processed at other temperatures (Figs. 4E-H).

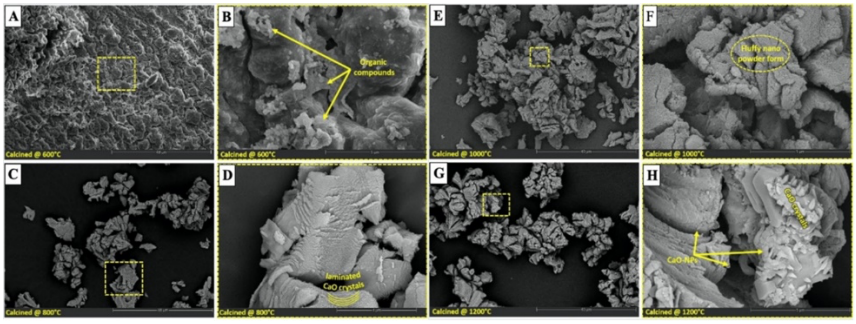

Figure 4. Surface morphology and microstructure of *P. caerulea* powder samples calcined at A-B) 600°C, C-D) 800°C, E-F) 1000°C and G-H) 1200°C.

6. Thermal Properties of *P. caerulea* Shell Powder

Equation [4] illustrates the thermal decomposition of calcium carbonate ($CaCO_3$) present in the *P. caerulea* shell, a process commonly referred to as calcination. This reaction involves the breakdown of $CaCO_3$ into calcium oxide (CaO) and carbon dioxide (CO_2) when subjected to high temperatures (Eq. 4).

$$CaCO_3(s) \rightarrow CaO(s) + CO_2(g) \quad (4)$$

Lime, an inorganic material, primarily consists of calcium oxide or calcium hydroxide compounds. Limestone, which is mainly composed of calcite, is the most prevalent carbonate rock from which calcite lime is derived [30,31]. Thermal gravimetric analysis (TGA) of *P. caerulea* shell powder (Fig. 5 - black line) reveals weight loss occurring in two distinct stages. Initially, thermal stability is maintained up to 655°C. Beyond this point, a significant mass loss (43.5 %) is observed between 655°C and 950°C, primarily attributable to the release of CO_2, consistent with the behavior expected of $CaCO_3$-based materials.

Differential thermal analysis (DTA) of the *P. caerulea* shell powder (Fig. 5 - blue line) shows minor endothermic peaks at 125°C and 275°C. The first peak likely corresponds to the evaporation of residual absorbed moisture, while the second peak is attributed to the release of organic matter residues absorbed within the *P. caerulea* sample.

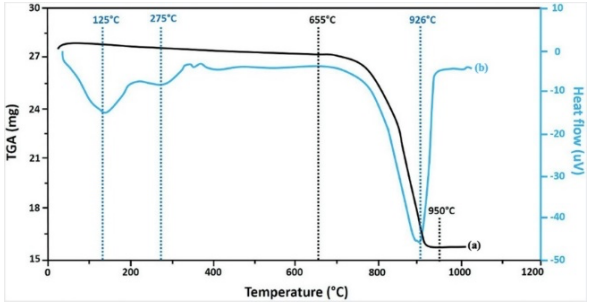

Figure 5. Thermal analysis curves of *P. caerulea* samples. (a) Gravimetric thermal analysis (TGA), (b) Differential thermal analysis (DTA).

7. X-ray diffraction (XRD) Analysis

X-ray diffraction (XRD) analysis was conducted to identify the mineral species of the calcined *P. caerulea* shells using an X-ray diffractometer [Malvern Panalytical EMPYREAN 3rd Generation Analytical (UK)] with Ni-filtered Cu-Kα radiation at 40 kV and 30 mA. The crystal structures and phases of calcined *P. caerulea* powders at various temperatures (600°C to 1200°C) were analyzed using XRD and are presented in Fig. 6. Powders calcined at 600°C exhibited four main characteristic peaks at diffraction angles (2θ°) of approximately 29.49°, 35.98°, 43.16°, and 47.11°, with corresponding Miller indices of (1 0 4), (1 1 0), (2 0 2), and (0 2 4), respectively. These peaks indicate the presence of $CaCO_3$ crystallized in the hexagonal calcite phase, as identified using PDF card number 47-1743. This finding is consistent with previous literature, such as the study by Soisuwan (2014), which identified the calcite ($CaCO_3$) crystalline structure in oyster shells through XRD analysis. Similarly, Park et al. [33] reported that oyster shells calcined at lower temperatures exhibited a hexagonal crystal structure.

At temperatures exceeding 600°C, the XRD patterns of the calcined *P. caerulea* powders displayed a similar trend. The highest intensity peaks were observed at diffraction angles (2θ°) of approximately 32.25°, 37.45°, 53.85°, and 64.15°, with corresponding Miller indices of (1 1 1), (2 0 0), (2 2 0) and (3 1 1). These peaks indicate the presence of a cubic calcium oxide (CaO) structure, as identified using PDF card number 48-1467. This analysis indicates that the primary component of *P. caerulea* shells calcined at 600°C was calcium carbonate ($CaCO_3$), whereas shells calcined at higher temperatures predominantly consisted of calcium oxide (CaO). In other words, the heat treatment at 600°C did not fully convert the $CaCO_3$ in *P. caerulea* shells into CaO. Conversely, heat treatments at 800°C, 1000°C, and 1200°C effectively transformed $CaCO_3$ into CaO. Additionally, it was observed that at calcination temperatures above 800°C, there was a small increase in the intensity of CaO peaks in the XRD spectra (Fig. 6).

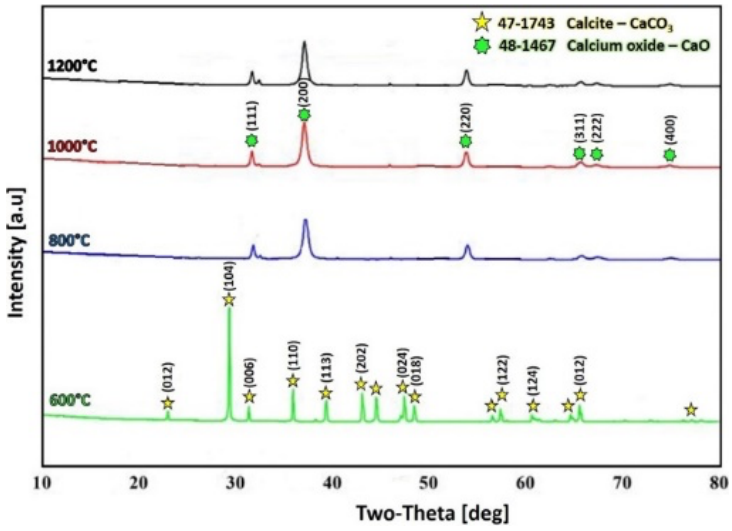

Figure 6. XRD spectra of calcined *P. caerulea* shell at different calcination temperatures.

8. Microwave radome applications

The objective is to promote the utilization of *P. caerulea* shells gathered from the Iskenderun shores across various domains. An exploration was undertaken to assess the viability of employing *P. caerulea* shells in microwave radome applications, involving their incineration at different temperatures. The study delved into the complex dielectric parameters of biomaterials derived from marine shells within the frequency range of 1 to 20 GHz, employing the open-ended coaxial probe method.

In Fig. 7, the measured values of real and imaginary components of diverse shell samples are depicted. Specifically, at the central frequency of 10 GHz, the real permittivity values for P600, P800, P1000 and P1200 are 3.2, 2.3, 2.4 and 2.5, respectively. Correspondingly, the imaginary parts for the same samples at 10 GHz are 0.82, 0.44, 0.52 and 0.56, reflecting variations attributable to the diverse heating temperatures applied. It is noteworthy that air exhibits an anticipated pattern with values of 1 for the real part and 0 for the imaginary part of the complex permittivity μ.

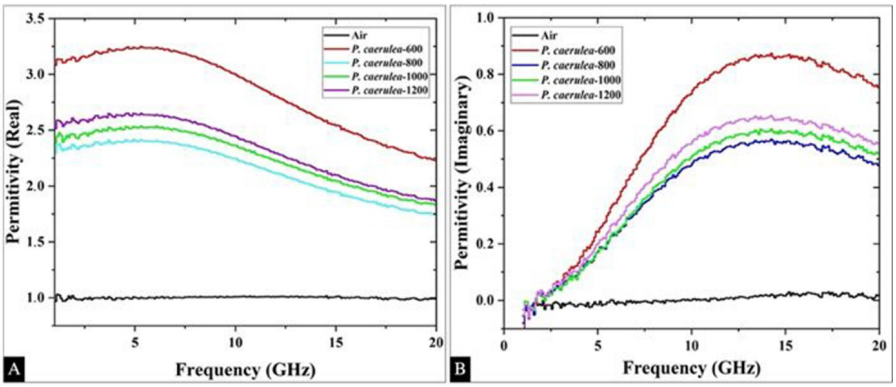

Figure 7. Real (A) and Imaginary (B) parts of measured *P. caerulea* samples in frequency range of 1-20 GHz

Although studies on the use of marine animals in radome applications are quite limited, when looking at the literature, there is only one previous study on marine crustacean species [19]. Shells and spines of the invasive sea urchin were used in this study. As a result of this study, it is clearly shown that the invasive sea urchin is a good candidate in microwave applications especially for radome integrations. According to the literature review, the results determined in previous traditional studies with radome applications are as given in Table 1. Table 1 presents the studies on dielectric measurements of various organic materials in microwave regions. These proposed materials can be used in microwave systems as substrate, dielectric resonator, and radome. As clearly shown in Fig. 7, P600, P800, P1000 and P1200 have 3.2, 2.3, 2.4 and 2.5 real dielectric constant at 10 GHz. In contrast, they have 0.82, 0.44, 0.52 and 0.56 imaginary dielectric constant at 10 GHz.

Table 1. Literature studies on dielectric measurements.

Material	Operating Frequency (GHz)	Aim application	Reference
Toxic marine invaders (*Diadema setosum*)	3.2-20	Radome	[19]
Polybutylene succinate (PBS)	2.3-11.7	Antenna substrate	[34]
Rice husk, rice straw, sugar cane bagasse and banana leaves	1-20	As a substrate material in microwaves	[35]
Methanol, ethanol, glycol, xylene	4.5	Not specified	[36]
Carbon teteachloride, carboncloroetylene, acetone, alcohol, heptane, toluene	0.2-20	Material sciences	[37]
Coal	2.216	Not specified	[38]
Teflon, wood, paper, white corn, yellow corn, sorghum	2.4-2.5	Not specified	[39]
Apple pulp waste	3-18	Absorbers	[40]
Calcined *P. caerulea* shells	1-20	Radome and substrate	***This study***

To show the feasible application area in microwave region, a traditional patch antenna is modelled and numerically analyzed. In this antenna configuration, the proposed P600, P800, P1000, and P1200 samples were

systematically integrated into the antenna layer within simulations to evaluate their feasibility for microwave system applications. The integration process accounted for material compatibility, dielectric properties, and potential interface losses to ensure a realistic representation of performance in practical implementations. The modelled antenna structure is shown in Fig. 8A which used P600, P800, P1000 and P1200 as dielectric substrate layer with 1mm thickness. This antenna design aims to operate at around 10GHz region that is between 6GHz and 14GHz frequency band. Fig. 8B illustrates the obtained return loss (S11) characteristics under different type of substrate materials. As shown, P600 has two resonance peaks at 7GHz and 12.4GHz with nearly -15dB and -13dB return loss values. Another material which is P800 shows resonance point at 10GHz with -23dB return loss value. Similarly, P1000 and P1200 has resonance at around 9.1GHz and 8.6GHz with -33dB and -23dB return loss values, respectively. These differences caused by the dielectric constant variations caused by calcined shell temperatures. This material is a good candidate for microwave antenna applications especially as a substrate layer which is given in Fig. 5 as an example.

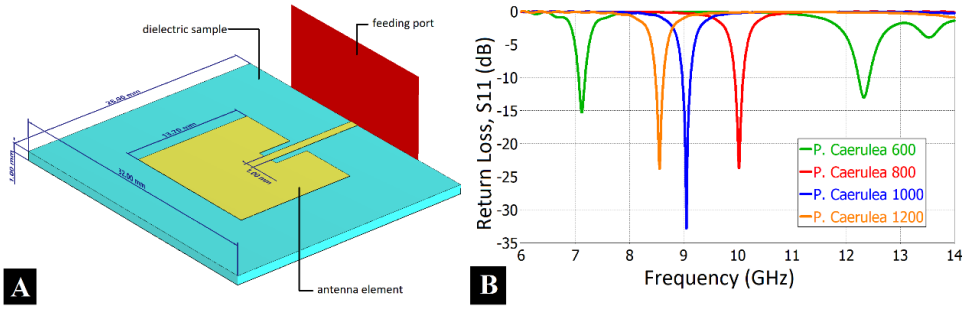

Figure 8. Patch antenna element (A) and Return Loss characteristics (B).

In addition, the loss factor of *P. caerulea* shells are in low level for low frequency region especially 2.5 GHz as illustrated in Figure 7. This loss level shows the application potential of *P. caerulea* shells in communication application such as microwave laminate fabrication and radome applications especially given in Fig. 8. The outcomes derived from complex permittivity measurements demonstrate that powdered materials from *P. caerulea* shells are highly promising for applications in microwave technology, particularly as substrate layers. These materials exhibit favorable low-loss characteristics, rendering them suitable for a spectrum of research applications, including but not limited to military radar, sensors, communication systems and medical applications.

9. Conclusion

This study delves into the microwave constitutive parameters of a biomaterial within the 1-20 GHz range, specifically focusing on calcined *P. caerulea* shells. These powder samples, derived from *P. caerulea* shells, were meticulously prepared at varying temperatures: 600, 800, 1000, and 1200°C. The process involved grinding the shells to transform them into powder. According to the SEM analysis results, the calcined *P. caerulea* shell powders exhibited a broad and rough structure at 600 °C. At 800 °C, surfaces with irregular shapes, roughness, and pores were recorded. As the temperature increased, the formation of CaO commenced, resulting in the formation of more pores. The morphology of CaO diverged from $CaCO_3$, displaying a dense, rough, and porous appearance between 1000°C and 1200 °C. Analysis revealed that *P. caerulea* shells calcined at 600 °C primarily consisted of $CaCO_3$, while those at other temperatures were mainly composed of CaO. However, at 800, 1000, and 1200 °C, $CaCO_3$ successfully transformed into CaO, with a slight increase in CaO peaks observed in the XRD spectrum at temperatures above 800°C.

Employing the open-ended coaxial probe method, the complex dielectric parameters of these categorized biomaterials were thoroughly investigated across the 1-20 GHz frequency spectrum. The measured dielectric results unequivocally indicate the significant potential of this biomaterial in the microwave frequency domain. The complex permittivity properties obtained from the measurements indicate that the proposed samples have significant potential for high-performance microwave applications. Their excellent impedance matching with air and low-loss characteristics make them promising candidates for microwave substrates, radomes, and the design of microwave circuits and resonators. While research on the microwave constitutive parameters of materials derived from marine invertebrates for antenna isolation remains limited, no prior studies have specifically explored the applicability of *P. caerulea*, a species abundantly found in the Mediterranean Sea, for radome technology. This

study, therefore, represents a pioneering effort in this field, filling a critical gap in the literature and demonstrating the feasibility of *P. caerulea* shells as a novel biomaterial for microwave applications.

Acknowledgment

The authors are thankful to the Center Laboratory of Iskenderun Technical University for providing the facility to carry out the work.

References

[1] Casal G, Aceña-Matarranz S, Fernández-Márquez D, Fernández N. Distribution and abundance patterns of three coexisting species of Patella (Mollusca Gastropoda) in the intertidal areas of the NW Iberian Peninsula: Implications for management, Fish Res 2018; 198: 86–98.
[2] Jenkins S, Coleman R, Burrows M, Hartnoll RG, Hawkins S. Regional scale differences in determinism of limpet grazing effects, Mar Ecol Prog Ser 2005; 287: 77–86.
[3] Prusina I, Peharda M, Ezgeta-Balic D, Puljas S, Glamuzina B, Golubic S. Life-history trait of the Mediterranean keystone species Patella rustica: growth and microbial bioerosion, Medit Mar Sci 2015; 16: 393.
[4] Hawkins SJ, Hartnoll RG, Grazing of intertidal algae by marine invertebrates, Oceanogr Mar Biol 1983; 21: 195–282.
[5] Arrontes J, Arenas F, Fernández C, J Rico, Oliveros J, Martínez B, Viejo R, Alvarez D. Effect of grazing by limpets on mid-shore species assemblages in northern Spain, Mar Ecol Prog Ser 2004; 277: 117–133.
[6] Moore P, Thompson RC, Hawkins SJ. Effects of grazer identity on the probability of escapes by a canopy-forming macroalga, J Experimen Mar Biol Ecol, 2007; 344: 170–180.
[7] Parpagnoli D, Pecchioli S, Santini G. Temporal determinants of grazing activity in the Mediterranean limpet *Patella caerulea*, Ethol Ecol Evol, 2013; 25: 388–399.
[8] Mauro A, Arculeo M, Parrinello N. Morphological and molecular tools in identifying the Mediterranean limpets Patella caerulea, Patella aspera and Patella rustica, J Experimen Mar Biol Ecol 2003; 295: 131–143.
[9] Bouzaza Z, Mezali K. Discriminant-based study of the shell morphometric relationships of Patella caerulea (Gastropoda: Prosobranchia) of the western Mediterranean Sea, Turk J Zool 2018; 42: 513–522.
[10] Vafidis D, Drosou I, Demetriou K, Klaoudatos D. Population Characteristics of the Limpet Patella caerulea (Linnaeus, 1758) in Eastern Mediterranean (Central Greece), Water 2020; 12: 1186.
[11] Navarro PG, Ramírez R, Tuya F, Fernandez-gil C, Sanchez-jerez P, Haroun RJ. Hierarchical Analysis Of Spatial Distribution Patterns Of Patellid Limpets In The Canary Islands, J Mollusc Stud 2005; 71: 67–73.
[12] Espinosa F, Guerra-García JM, Fa D, García-Gómez JC. Effects of competition on an endangered limpet Patella ferruginea (Gastropoda: Patellidae): Implications for conservation, J Experimen Mar Biol Ecol 2006; 330: 482–492.
[13] Paulo Cabral J. Shape and growth in European Atlantic Patella limpets (Gastropoda, Mollusca). Ecological implications for survival, Web Ecol 2007; 7: 11–21.
[14] Prusina I, Ezgeta-Balić D, Ljubimir S, Dobroslavić T, Glamuzina B. On the reproduction of the Mediterranean keystone limpet *Patella rustica* : histological overview, J Mar Biol Ass 2014; 94: 1651–1660.
[15] Duysak Ö, Azdural K. Evaluation of heavy metal and aluminium accumulation in a gastropod, patella caerulea L., 1758 in Iskenderun Bay, Turkey, Pak J Zool 2017; 49: 629–637.
[16] Küçükdermenci A, Lök A, Kirtik A, Kurtay E. The meat yield variations of Patella caerulea (Linnaeus, 1758) in Urla, Izmir Bay, Acta Biol Tur 2017; 30: 174–177.
[17] Yücel N, Kılıç E. Presence of microplastic in the Patella caerulea from the northeastern Mediterranean Sea, Mar Poll Bull 2023; 188: 114684.
[18] Uğurlu E. Using Patella caerulea as a biomaterial: Chitin and Chitosan, AUJES 2023; 4: 394–405.
[19] Uğurlu E, Duysak Ö, Alkurt FÖ, Karaaslan M, Franco AP. Utilization of Poisonous Marine invader in Development of Low Losses Microwave Devices, NÖHÜ Müh Bilim Derg 2023; 12: 1335–1340.
[20] Geng H, Chen M, Guo C, Wang W, Chen D. Marine polysaccharides: Biological activities and applications in drug delivery systems, Carbohydr Res 2024; 538: 109071.
[21] Shavit R. Radome electromagnetic theory and design, John Wiley & Sons, 2018.
[22] Panwar R, Lee JR. Performance and non-destructive evaluation methods of airborne radome and stealth structures, Meas Sci Technol 2018; 29: 062001.
[23] Gorgucci E, Bechini R, Baldini L, Cremonini R, Chandrasekar V. The Influence of Antenna Radome on Weather Radar Calibration and Its Real-Time Assessment, J Atmos Ocean Tech 2013; 30: 676–689.
[24] Yu J, Zhang K, Duan M, Lv W, Zhang X. Study on the stability of air traffic control radar radome under wind Load, IEEE, 2023: 1152–1155.
[25] Xing Z, Yang F, Yang J, Zhu X. Low-RCS Ka-band receiving and transmitting satellite communication antennas co-designed with high-performance absorbent frequency-selective radomes, J Electromagn Waves Appl 2023; 37: 190–206.
[26] Park HJ, Jeong SW, Yang JK, Kim BG, Lee SM. Removal of heavy metals using waste eggshell, J Environ Sci 2007; 19: 1436–1441.

[27] Öksüz KE. Sert Doku Uygulamaları İçin Makro Gözenekli Alüminyum Oksit-Bor Karbür Seramikleri, RTEUFEMUD 2023; 4: 65–75.
[28] Kaatze U. Techniques for measuring the microwave dielectric properties of materials, Metrologia 2010; 47: S91–S113.
[29] Gabriel C, Gabriel S, Grant EH, Grant EH, Halstead BSJ, Michael D, Mingos P. Dielectric parameters relevant to microwave dielectric heating, Chem Soc Rev 1998; 27: 213.
[30] Öksüz KE, Şereflişan H. Microstructure of Eobania vermiculata (Müller, 1774): SEM, F-TIR and XRD Methods, J Agricul Product 2022; 3: 42–47.
[31] Ferraz E, Gamelas JAF, Coroado J, Monteiro C, Rocha F. Recycling Waste Seashells to Produce Calcitic Lime: Characterization and Wet Slaking Reactivity, Waste Biomass Valor 2019; 10: 2397–2414.
[32] Soisuwan S, Phommachant J, Wisaijorn W, Praserthdam P. The Characteristics of Green Calcium Oxide Derived from Aquatic Materials, Procedia Chem 2024; 9: 53–61.
[33] Park K, Sadeghi K, Thanakkasaranee S, Park Y, Park J, Nam K, Han H, Seo J. Effects of calcination temperature on morphological and crystallographic properties of oyster shell as biocidal agent, Int J Applied Ceramic Tech 2021; 18: 302–311.
[34] Habib Ullah M, Mahadi WNL, Latef TA. Aerogel Poly (butylene succinate) Biomaterial Substrate for RF and Microwave Applications, Sci Rep 2015; 5: 12868.
[35] Zulkifli NA, Wee FH, Mahrom N, Yew BS, Lee YS, Ibrahim SZ, Am Phan AL. Analysis of Dielectric Properties On Agricultural Waste for Microwave Communication Application, MATEC Web Conf 2017; 140: 01013.
[36] Sekar V, Torke WJ, Palermo S, Entesari K. A Self-Sustained Microwave System for Dielectric-Constant Measurement of Lossy Organic Liquids, IEEE Trans. Microwave Theory Techn 2012; 60: 1444–1455.
[37] Zarubina AY, Kibets SG, Politiko AA, Semenenko VN, Baskov KM, Chistyaev VA. Complex permittivity of organic solvents at microwave frequencies, in: IOP Publishing, 2020: p. 062085.
[38] Marland S, Merchant A, Rowson N. Dielectric properties of coal, Fuel 2001; 80: 1839–1849.
[39] Hernandez-Gomez ES, Olvera-Cervantes JL, Corona-Chavez A, Sosa-Morales ME. Development of a low cost dielectric permittivity sensor for organic and inorganic materials in the microwave frequency range, in: 2014 IEEE 9th IberoAmerican Congress on Sensors, IEEE, Bogota, Colombia, 2014: pp. 1–4.
[40] Baltacioğlu K, Başar M, Karaaslan M, Alkurt F, Aripek S, Electromagnetic Analysis of Organic Waste and Blust Furnace Slag Mixtures, Eur Mech Sci 2021; 5: 148–152.